Dynamic stability in hovering flight of insects with different sizes

Yu Zhu Lyu and Mao Sun*
Institute of Fluid Mechanics, Beihang University, Beijing 100191, China

(Received 24 December 2021; accepted 16 April 2022; published 6 May 2022)

Previous works on the flight dynamic stability of insects have focused on relatively large insects. Here, the longitudinal flight dynamic stability of two hovering miniature insects was computed. With the stability properties of the miniature insects from the present work and those of large insects from previous works, we studied the effects of insect size on the stability properties in the full range of insect sizes. The following results were obtained. Although the insects considered have a 30 000-fold difference in mass, their modal structure of flight stability is the same: an unstable oscillatory mode, a stable fast subsidence mode, and a stable slow subsidence mode; because of the unstable mode, the flight is unstable. An approximate analytical expression on the growth rate of the unstable mode as a function of insect mass (m) was derived. It shows that the time to double the initial values of disturbances (t_d) is proportional to the 0.17 power of the insect mass (m). That is, as m becomes smaller, t_d decreases (i.e., the instability becomes faster). This means that miniature insects need a faster nervous system to control the instability than larger insects. For example, the response time (represented by t_d) of a miniature insect, the gall midge ($m \approx 0.05$ mg), needs to be faster by about 7 times than that of a larger insect, the hawk moth ($m \approx 1600$ mg).

DOI: 10.1103/PhysRevE.105.054403

I. INTRODUCTION

The size and mass of flying insects change greatly among different species [1]. The mass difference between the largest and the smallest insects is as large as five orders of magnitude (e.g., the mass of a large insect, the hawk moth *Manduca sexta*, is more than 1.6 g, whereas that of a miniature insect, the small wasp *Encarsia formosa*, is less than 0.016 mg) [2–6]. With such a wide range of mass difference, exploring the effect of insect size on the flight dynamic stability must be very interesting.

Flight dynamic stability and stabilization control are of great importance in the study of biomechanics of insect flight. Much work has been done in those areas (e.g., Refs. [7–15]). Taylor and Thomas [7] did the first quantitative analysis on the stability of an insect (desert locust). They used the averaged model and linear analysis. Because they determined the stability derivatives by experiments using real insects, and the results inevitably included some control effects, the inherent stability properties of the insect were not obtained. Other researchers avoided this problem by using insect models for computing or measuring the stability derivatives. Sun and Xiong [8] and Faruque and Humbert [10,11] studied the dynamic stability problem of a bumblebee. Cheng and Deng [13] studied the same problem for a number of insects, including hawk moth, bumblebee, stalk-eyed fly, and fruit fly. The stability properties of several other insects, including hover fly, drone fly, crane fly and mosquito, were also obtained [16–20]. Dickson *et al.* [21], Sun and Wang [22], Ristroph *et al.* [23,24] and Cheng *et al.* [25] added the control terms into the linearized averaged model, and studied the stabilization control problem of several insects. Wu and Sun [26] and Noest and Wang [27] extended the analysis based on the averaged model to the Floquet analysis, so that problems with large effect of wing-body coupling could be treated. Chang and Wang [28] developed a model in which the dynamics is governed by full nonlinear equations, and studied the fruit fly's flight stabilization problems; since there is not linearization, large disturbance motion can be treated by their model.

The mass of the above insects studied in the above works, for which the stability properties are available, ranges from about 1.6 g (hawk moths) to about 1 mg (mosquitoes and fruit flies). This covers the mass range of many winged insects, except that of the miniature insects whose mass is more than one order of magnitude smaller. One reason for the absence of the stability analysis of miniature insects is that their wing flapping kinematics data were not available. Recently, the wing kinematics parameters for a number of miniature insects were measured [29–31]. Now the stability properties of miniature insects can be calculated. If this is done, the effect of insect size on the flight dynamic stability can be analyzed in the full range of insect size.

In the present study, as a first step, we will consider the longitudinal flight stability problem of hovering insects. First, we will compute the stability properties of some miniature insects, i.e., vegetable leaf miner (*Liriomyza sativae*) and gall midge (*Anbremia* sp.); the mass of the vegetable leaf miner is 0.25 mg and that of the gall midge is 0.05 mg. Then, based on the computed results of the miniature insects and those of larger insects previously computed by our and other research groups, we will analyze the size effect on the flight dynamic stability. By making some reasonable simplifications, we will try to obtain some simple equations showing the effect of size (mass) on the stability properties.

*m.sun@buaa.edu.cn

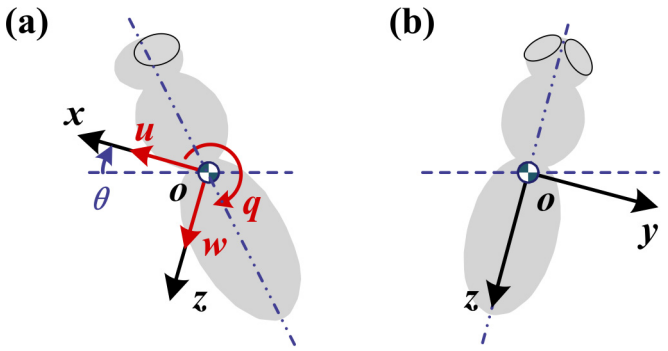

FIG. 1. The state variables and the reference frames: (a) Side view; (b) back view.

II. MATERIALS AND METHODS

A. Methods for the stability analysis of the miniature insects

The averaged-model theory [7,8] is used in the analysis. In the model, the insect is represented by a rigid body that has six degrees of freedom; the action of the back-and-forth beating wings is represented by the wingbeat-cycle-average forces and moments. As a result, the equations of motion of the insect become the same form as those of airplanes. For studying the stability study, we use the linear-analysis method: The equations of motion are linearized by approximating the body's motion as small disturbances from a reference (equilibrium) condition.

Let $oxyz$ be a noninertial right-handed coordinate system fixed to the body. The origin o is at the center of mass of the insect and the axes are aligned so that at equilibrium flight, the x and y axes are horizontal, the x axis points forward, and the y axis points to the right of the insect (Fig. 1). The variables that define the longitudinal disturbance motion are as follows: the components of velocity of the center of mass along the x axis (denoted as u) and the z axis (denoted as w) (Fig. 1), the components of the body angular velocity around the y axis (denoted as q, called pitch velocity) (Fig. 1), and the pitch angle (denoted as θ) (Fig. 1). Let m denote the mass of the insect, g denote the gravitational acceleration, and I_y denote the moment of inertia about the y axis. The x and z components of the mean aerodynamic force are represented by X and Z, respectively; the mean aerodynamic moment around the y axis is represented by M_y. When the insect is hovering, at reference flight, u, w, and q are all zero, and the force and moment components are also zero except that Z balances the insect weight. The small-disturbance equations of motion are as follows [32]:

$$\begin{bmatrix} \delta\dot{u}^+ \\ \delta\dot{w}^+ \\ \delta\dot{q}^+ \\ \delta\dot{\theta} \end{bmatrix} = \mathbf{A}^+ \begin{bmatrix} \delta u^+ \\ \delta w^+ \\ \delta q^+ \\ \delta\theta \end{bmatrix}, \tag{1}$$

$$\mathbf{A}^+ = \begin{bmatrix} \frac{X_u^+}{m^+} & \frac{X_w^+}{m^+} & \frac{X_q^+}{m^+} & -g^+ \\ \frac{Z_u^+}{m^+} & \frac{Z_w^+}{m^+} & \frac{Z_q^+}{m^+} & 0 \\ \frac{M_u^+}{I_y^+} & \frac{M_w^+}{I_y^+} & \frac{M_q^+}{I_y^+} & 0 \\ 0 & 0 & 1 & 0 \end{bmatrix}. \tag{2}$$

The superscript "+" represents a dimensionless quantity. The symbol δ denotes a small-disturbance quantity and the overdot represents the time derivative; X_u, Z_u, etc., are the stability derivatives representing partial derivatives of the forces and moments with respect to the motion variables. When nondimensionalizing the equations, for the variables, the mean chord length of the wing c is the length scale, the period of the wingbeat cycle $T = 1/n$ is the timescale, and the mean wingbeat velocity $U = 2\Phi n r_2$ is the velocity scale (here Φ is the wingbeat amplitude, n is the wingbeat frequency, and r_2 is the radius of gyration of the wing). A force, e.g., X, is nondimensionalized by $\rho U^2 S/2$, where ρ is the air density and S the area of the wing pair, and a moment, e.g., M, is nondimensionalized by $\rho U^2 Sc/2$. In addition, an inertia moment is nondimensionalized by $\rho U^2 ScT^2/2$, time by T, mass by $\rho UST/2$, and gravitational acceleration (g) by U/T. The matrix $\boldsymbol{A}$ is called the system of matrix. To solve Eq. (1), the elements in $\boldsymbol{A}$ need to be known. That is, m, I_y and X_u, Z_u, etc., need to be known. How these quantities are determined is discussed in Appendixes A and B.

Once $\boldsymbol{A}$ is specified, Eq. (1) can be solved to yield insights into the dynamic flight stability of the hovering insect. The central elements of the solutions for the dynamic stability problem are the eigenvalues and eigenvectors of $\boldsymbol{A}$ (Ref. [32]). Here $\boldsymbol{A}$ has four eigenvalues (λ_1, λ_2, λ_3, λ_4) and four corresponding eigenvectors. A real eigenvalue and the corresponding eigenvector, or a conjugate pair of complex eigenvalues and the corresponding eigenvector pair, represent a natural mode of the system. The motion of the flying body after an initial deviation from its reference flight is a linear combination of the natural modes. In a natural mode, the real part of the eigenvalue determines the time rate of growth of the disturbance quantities and the eigenvector determines the magnitudes and phases of the disturbance quantities relative to each other. A positive real eigenvalue will result in exponential growth of each of the disturbance quantities, so the corresponding natural mode is dynamically unstable (termed unstable divergent mode). The time to double the starting value (t_d) is given by $t_d = 0.693/\lambda$ ($\lambda > 0$). A pair of complex conjugate eigenvalues, e.g., $\lambda_{1,2} = s \pm \omega i$, will result in oscillatory time variation of the disturbance quantities with ω as its angular frequency. The motion decays when s is negative (dynamical stable, termed stable oscillatory mode) but grows when s is positive (dynamical unstable, termed unstable oscillatory mode). The time to double the oscillatory amplitude is $t_d = 0.693/s$.

It should be noted that in the above analysis method, the equation of motion and the aerodynamic forces and moments are linearized about the reference point (equilibrium flight). This means that our results are valid only for the cases in which the disturbance motions are small.

B. Method for studying the effects of insect size (mass)

As mentioned above (see Sec. II A), the stability properties (the mode structure, a mode being stable or unstable, the growth or decay rate of a mode, etc.) are determined by the eigenvalues of the system matrices $\boldsymbol{A}$. The eigenvalues are the roots of the characteristic equation of $\boldsymbol{A}$. The characteristic

equation of $\boldsymbol{A}$ can be written as

$$\begin{bmatrix} \frac{X_u^+}{m^+} - \lambda^+ & \frac{X_w^+}{m^+} & \frac{X_q^+}{m^+} & -g^+ \\ \frac{Z_u^+}{m^+} & \frac{Z_w^+}{m^+} - \lambda^+ & \frac{Z_q^+}{m^+} & 0 \\ \frac{M_u^+}{I_y^+} & \frac{M_w^+}{I_y^+} & \frac{M_q^+}{I_y^+} - \lambda^+ & 0 \\ 0 & 0 & 1 & 0 \end{bmatrix} = 0, \quad (3)$$

which is an algebraic equation of fourth order. Its roots have very complex expressions, and from their expressions, it is virtually impossible to see the effects of insect size (mass) on the roots. But this problem might be overcome in the following way.

From the results of previous studies on many insects, we found that some stability derivatives are much smaller than others, for example, X_w^+ is much smaller than X_u^+ and X_q^+. This means that dropping the terms with these small derivatives could give simpler characteristic equations and simpler expressions of the roots (eigenvalues), without losing too much of the accuracy of the roots. With the simplified expressions of the roots, it is easier to see the effects of insect size (mass).

In the present study, we will use the above approach and try to obtain simple expressions for the eigenvalues, so that the effects of insect size can be clearly seen. Furthermore, we try to give a simple formula that can show how the insect size (mass) affects the growth rate of the unstable mode; this quantity is of great importance to the study of the control system of an insect.

III. RESULTS ON THE TWO MINIATURE INSECTS

A. Computed stability derivatives

As discussed in the calculation of stability derivatives in Appendix B, forces and moment for each of u, w, etc., varying independently from their equilibrium value are calculated and the corresponding nondimensional aerodynamic forces and moments on the wings X^+, M^+, etc., are obtained, giving ΔX^+, ΔM^+, etc. As an example, the u-series, w-series, and q-series results of ΔX^+, ΔZ^+, and ΔM^+ of the gall midge are plotted in Fig. 2. The variations of ΔX^+, ΔZ^+, and ΔM^+ have good linearity, showing that for small-disturbance motion, linearization of the aerodynamic forces and moments is justified. The curves in the figure are fitted separately by straight lines, which give the stability derivatives X_u^+, Z_u^+, etc. The estimated stability derivatives of the two small insects are shown in Table I.

As seen in Table I, the derivatives of the two insects are generally similar: The magnitudes of X_u^+, M_u^+, and Z_w^+ are larger than those of the other derivatives. The value of X_u^+ is negative and that of M_u^+ is positive; this means that the horizontal translation produces a horizontal damping force (negative X_u^+; the force is opposing the motion) and a pitching moment that tilts the insect in the opposite direction of the translation motion. The value of Z_w^+ is negative, indicating that vertical motion produces a vertical force opposing the motion. There are also some differences in the derivatives between the two insects: the magnitudes of X_u^+, Z_u^+, Z_w^+, and M_w^+ of the gall midge are larger than those of their counterparts of the vegetable leaf miner. These differences are due to the difference in wing motion pattern between the two insects: the vegetable leaf miner has a shallow U-shape upstroke, while the gall midge uses a deep U-shape upstroke [29]. As will be seen in a later section (Sec. IV A), the nondimensional longitudinal derivatives of the two insects (especially the vegetable leaf miner) are very similar to those of larger insects.

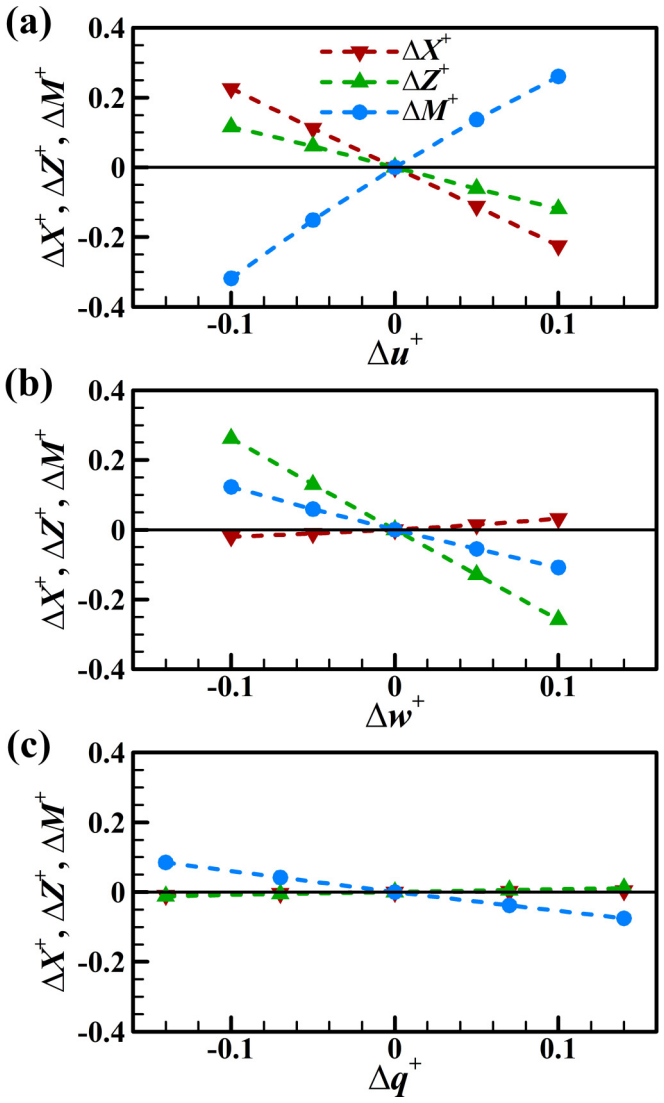

FIG. 2. The u-series, w-series, and w-series force and moment data for the gall midge.

TABLE I. Stability derivatives of the miniature insects.

Species	X_u^+	Z_u^+	M_u^+	X_w^+	Z_w^+	M_w^+	X_q^+	Z_q^+	M_q^+
Vegetable leaf miner (*Liriomyza sativae*)	−1.55	−0.43	4.37	0.26	−0.90	0.00	−0.18	0.11	−0.33
Gall midge (*Anbremia* sp.)	−2.25	−1.19	2.89	0.26	−2.60	−1.14	0.04	0.08	−0.57

TABLE II. Eigenvalues of the miniature insects.

Species	Mode 1 λ_1^+, λ_2^+	Mode 2 λ_3^+	Mode 3 λ_4^+
Vegetable leaf miner (*Liriomyza sativae*)	$0.11 \pm 0.24i$	-0.30	-0.014
Gall midge (*Anbremia* sp.)	$0.12 \pm 0.28i$	-0.46	-0.13

B. Dynamic stability properties

With the stability derivatives calculated in the previous section (Sec. III A) and the insect mass and the moments and product of inertia determined in Appendix A, elements in $\boldsymbol{A}$ of the equations of motion, Eq. (1), are now known. We are ready to compute the eigenvalues and eigenvectors of $\boldsymbol{A}$ and obtain the stability properties of the two small insects. The computed results are given in Table II (eigenvalues) and Table III (eigenvectors).

As seen from the eigenvalues in Table II, for the disturbance motion, there is a pair of complex eigenvalues, λ_1^+ and λ_2^+, which have a positive real part, and there are two negative real eigenvalues (λ_3^+ and λ_4^+; the magnitude of λ_3^+ is relatively large and that of λ_4^+ is relatively small), one with a large magnitude and the other with a small magnitude. Therefore, the longitudinal motion has three natural modes: an unstable oscillatory mode (referred to as mode 1), a stable fast subsidence mode (referred to as mode 2) and a stable slow subsidence mode (referred to as mode 3). From the eigenvectors (Table II), it is seen that mode 1 and mode 2 contain the horizontal (δu) and vertical (δw) motions and pitching (δq) rotation, and mode 2 mainly has horizontal (δu) and vertical (δw) motions (δq is about one order of magnitude smaller than δu and δw). Owing to the unstable mode 1, the longitudinal motion of the gall midge is unstable.

The modal structures of the two small insects (gall midge and vegetable leaf miner) are similar to those of other larger insects studied in many previous works (e.g., Refs. [8–20]), having an unstable oscillatory mode (mode 1), a stable fast subsidence mode (mode 2) and a stable slow subsidence mode (mode 3). The longitudinal motion is unstable due to the existence of the unstable mode 1.

IV. SIZE EFFECTS ON THE STABILITY PROPERTIES OF INSECTS

The stability properties of some miniature insects have been obtained in the above section (Sec. III); those of many larger insects are available from the literature [8–20]. Now we have stability properties for the approximately full-size range of insects, m ranging from about 0.05 mg to about 1600 mg, a difference of five orders of magnitude, and we can examine the effect of size (mass) on the dynamic stability of insects for the full-size range.

A. Stability derivatives of insects of various size

The nondimensional stability derivatives of the insects of various size (mass) are listed in Table IV; for the two small insects, the values are from our calculations and for the large insects, the values are from various references (*Manduca sexta* 1 [13], *Manduca sexta* 2 [26], *Bombus terrestris* 1 [8], *Bombus terrestris* 2 [13], *Eristalis tenax* [26], *Episyrphus balteatus* [16], *Tipula obsolete* [16], *Cyrtodiopsis dalmanni* [13], *Drosophila virilis* [19], *Aedes aegypti* [20], and *Drosophila melanogaster* [13]). The largest insect, a hawk moth (*Manduca sexta*), has a mass of 1620 mg and the smallest insect, a gall midge (*Anbremia* sp.), has a mass of 0.047 mg, a more than 30 000-fold mass difference. In the above cited works, for the calculation of the stability derivatives (and the eigenvalues), measured wing motion and morphology for each insect were used for the same insect. For example, for the hawk moths in Refs. [13,26], data measured by Ellington [2,33] were used; for the bumblebees in Refs. [8,13], data measured by Dudley and Ellington [34] were used.

First, let us look at the longitudinal stability derivatives in Table IV. The following observations can be made. The first is that for each of the insects here, large or small, the magnitudes of the derivatives X_u^+, M_u^+, and Z_w^+ are much larger than those of the other longitudinal derivatives. The second observation is that although the mass difference of the insects is very large (different by five orders of magnitudes), the magnitudes of the nondimensional derivatives do not vary greatly. For example, the magnitude of X_u^+ of all the insects considered is about 1–2; even the insects have more than 30 000-fold mass difference. The third observation is that for all insects listed, M_u^+, which represents the pitching moment

TABLE III. Eigenvectors of the miniature insects.

Species		Mode 1	Mode 2	Mode 3
Vegetable leaf miner	δu^+	0.098 (120.4°)	0.093(0°)	0.235(180°)
	δw^+	0.002(−79.5°)	0.004(0°)	6.024(0°)
(*Liriomyza sativae*)	δq^+	0.264(65.6°)	0.303(180°)	0.014(180°)
	$\delta\theta$	1(0°)	1(0°)	1(0°)
Gall midge	δu^+	0.153(88.8°)	0.285(0°)	1.103(0°)
	δw^+	0.154(12.0°)	0.290(0°)	2.810 (0°)
(*Anbremia* sp.)	δq^+	0.308(66.8°)	0.464(180°)	0.162(180°)
	$\delta\theta$	1(0°)	1(0°)	1(0°)

TABLE IV. Stability derivatives of the insects of various sizes.

Species	m (mg)	X_u^+	Z_u^+	M_u^+	X_w^+	Z_w^+	M_w^+	X_q^+	Z_q^+	M_q^+
Manduca sexta 1	1620	−1.97	0	1.13	0	−1.51	0	0	0	−0.13
Manduca sexta 2	1579	−2.16	−0.10	1.61	0.10	−1.33	−0.22	−0.27	0.06	−0.05
Bombus terrestris 1	175	−0.79	−0.03	2.39	0.05	−1.03	−0.19	−0.09	−0.03	−0.88
Bombus terrestris 2	175	−1.79	0	1.74	0	−1.56	0	0	0	−0.19
Eristalis tenax	88.3	−1.25	0.01	1.59	0.02	−1.36	0.08	−0.18	0.04	−0.13
Episyrphus balteatus	27.3	−1.28	−0.04	2.32	0.01	−1.26	0.05	−0.16	0.00	−0.02
Tipula obsolete	11.4	−1.09	−0.06	3.87	−0.01	−1.03	0.13	−0.09	0.01	−0.05
Cyrtodiopsis dalmanni	7.00	−1.52	0	2.52	0	−1.62	0	0	0	−0.31
Drosophila virilis	1.79	−1.48	−0.03	2.54	0.02	−1.64	−0.52	−0.06	0.14	−0.36
Aedes aegypti (female)	1.78	−1.43	−0.15	2.92	0.03	−1.63	0.31	−0.30	0.18	−0.41
Drosophila melanogaster	0.96	−1.48	0	0.92	0	−1.58	0	0	0	−0.19
Aedes aegypti (male)	0.82	−1.63	0.09	3.30	0.09	−1.85	−0.11	−0.45	0.51	−0.21
Liriomyza sativae	0.25	−1.55	−0.43	4.37	0.26	−0.90	0.00	−0.18	0.11	−0.33
Anbremia sp.	0.05	−2.25	−1.19	2.89	0.26	−2.60	−1.14	0.04	0.08	−0.57

produced by forward and backward motion, is positive; i.e., forward motion produces a pitching-up moment and backward motion produces a pitching-down moment. As discussed in our previous work [8], the sign of M_u^+ is very important in determining the natural modes.

B. Natural modes of motions (eigenvalues) of the insects

The eigenvalues of the insects are shown in Table V; again, for the two small insects, the values are from our calculations and for the large insects, the values are from various references (*Manduca sexta* 1 [13], *Manduca sexta* 2 [26], *Bombus terrestris* 1 [8], *Bombus terrestris* 2 [13], *Eristalis tenax* [26], *Episyrphus balteatus* [16], *Tipula obsolete* [16], *Cyrtodiopsis dalmanni* [13], *Drosophila virilis* [19], *Aedes aegypti* [20], and *Drosophila melanogaster* [13]).

It is seen from Table V that the model structure of the disturbance motion is the same for all the insects considered: An unstable oscillatory mode (mode 1), given by a pair of complex eigenvalues, λ_1^+ and λ_2^+; two stable subsidence modes (mode 2 and mode 3) given by two negative, real eigenvalues λ_3^+ and λ_4^+, respectively, one (mode 2) having a relatively fast decreasing rate ($|\lambda_3|$ is relatively large) and the other (mode 3) having a relatively slow decreasing rate ($|\lambda_3|$ is relatively small).

TABLE V. Eigenvalues of the insects of various sizes.

Species	Mode 1 λ_1^+, λ_2^+	Mode 2 λ_3^+	Mode 3 λ_4^+
Manduca sexta 1	0.17 ± 0.40i	−0.53	−0.09
Manduca sexta 2	0.25 ± 0.59i	−0.72	−0.094
Bombus terrestris 1	0.045 ± 0.13i	−0.20	−0.012
Bombus terrestris 2	0.06 ± 0.12i	−0.15	−0.02
Eristalis tenax	0.047 ± 0.094i	−0.11	−0.015
Episyrphus balteatus	0.074 ± 0.14i	−0.17	−0.020
Tipula obsolete	0.33 ± 0.73i	−0.87	−0.11
Cyrtodiopsis dalmanni	0.05 ± 0.11i	−0.13	−0.02
Drosophila virilis	0.082 ± 0.19i	−0.24	−0.027
Aedes aegypti (female)	0.023 ± 0.045i	−0.54	−0.008
Drosophila melanogaster	0.067 ± 0.14i	−0.18	−0.024
Aedes aegypti (male)	0.018 ± 0.036i	−0.044	−0.008
Liriomyza sativae	0.11 ± 0.24i	−0.30	−0.014
Anbremia sp.	0.12 ± 0.28i	−0.46	−0.13

Because of the unstable mode 1, the hovering flight of insects of all sizes considered here is intrinsically unstable. The flight must be actively controlled to be stable. That is, the insects need to constantly react to their surroundings and adjust their wing motion to control their body and keep from tumbling. The response time of the nervous system needs to be fast enough to react and keep the unstable mode from growing too large. Therefore, the growth rate of the unstable mode (mode 1) is of great interest. As previously mentioned (Sec. II A), t_d, the time to double the initial values of disturbances, represents the growth rate of instability. Therefore, let us examine size effect on this quantity.

From Sec. II A, $t_d = 0.693/s$; here the quantities are dimensional values (it is better to see the response time in real time). The values of t_d for the insects are plotted in Fig. 3. The following observations can be made from the data in Fig. 3. In general, t_d decreases when insect mass (m) decreases; as m

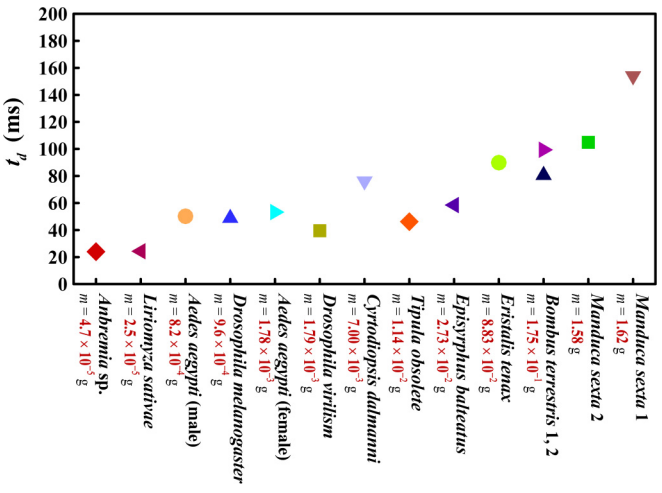

FIG. 3. The values of t_d for the insects of various size.

changes from about 1600 mg to about 0.05 mg, t_d changes from about 140 ms to about 20 ms. This means that for stable flight, smaller insects need faster nervous systems; the response time of a miniature insect ($m \approx 0.05$ mg) needs to be faster by about 7 times than that of the largest insect ($m \approx 1600$ mg).

C. Approximate expression for the t_d -mass relation

In the previous section (Sec. IV B), we have seen that t_d generally decreases when m decreases. It is desirable to have an analytical expression for t_d varying as a function of m. This could be achieved if we have analytical expressions for the eigenvalues. In a previous study performed by our group [16], it was shown that approximate analytical expressions for the eigenvalues could be obtained by introducing certain appropriate simplifications. Here we use the same method to obtain the expressions of the eigenvalues.

The characteristic equation of the system matrix $\boldsymbol{A}$ has been given in Eq. (3) in Sec. II, which is a fourth-order algebraic equation. From Table IV, we see that for each of the insects, $|X_w^+|$ is much smaller than $|X_u^+|$ and that $|M_w^+|$ is much smaller than $|M_u^+|$. Neglecting $|X_w^+|$ and $|M_w^+|$, Eq. (3) becomes

$$\begin{bmatrix} \frac{X_u^+}{m^+} - \lambda^+ & 0 & \frac{X_q^+}{m^+} & -g^+ \\ \frac{Z_u^+}{m^+} & \frac{Z_w^+}{m^+} - \lambda^+ & \frac{Z_q^+}{m^+} & 0 \\ \frac{M_u^+}{I_y^+} & 0 & \frac{M_q^+}{I_y^+} - \lambda^+ & 0 \\ 0 & 0 & 1 & 0 \end{bmatrix} = 0, \quad (4)$$

i.e.,

$$\left(\frac{Z_w^+}{m^+} - \lambda^+\right)\left[-\lambda^{+3} + \left(\frac{X_u^+}{m^+} + \frac{M_q^+}{I_y^+}\right)\lambda^{+2} + \left(\frac{X_q^+ M_u^+}{m^+ I_y^+} - \frac{X_u^+ M_q^+}{m^+ I_y^+}\right)\lambda^+ - \frac{g^+ M_u^+}{I_y^+}\right] = 0. \quad (5)$$

Equation (5) can be written as

$$-\lambda^{+3} + \left(\frac{X_u^+}{m^+} + \frac{M_q^+}{I_y^+}\right)\lambda^{+2} + \left(\frac{X_q^+ M_u^+}{m^+ I_y^+} - \frac{X_u^+ M_q^+}{m^+ I_y^+}\right)\lambda^+ - \frac{g^+ M_u^+}{I_y^+} = 0, \quad (6)$$

and

$$\frac{Z_w^+}{m^+} - \lambda^+ = 0. \quad (7)$$

That is, the fourth-order equation becomes a third-order equation, Eq. (6), and a first-order equation, Eq. (7). The exact expressions of the roots of Eq. (6) can be easily obtained, but the expressions are very complex and it is not easily to see how a parameter, for example, $|M_u^+|$, affects the roots. By using the expansion of binomial series (see Ref. [16]) and neglecting small terms of higher order (the higher-order small terms are due to the multiplication of some small derivatives), relatively simple approximate expressions of the roots of Eq. (6) can be obtained as

$$\lambda_{1,2}^+ = \frac{1}{2}\sqrt[3]{\frac{M_u^+ g^+}{I_y^+}}(1-2j) \pm i\frac{\sqrt{3}}{2}\sqrt[3]{\frac{g^+ M_u^+}{I_y^+}}, \quad (8)$$

$$\lambda_3^+ = -\sqrt[3]{\frac{g^+ M_u^+}{I_y^+}}(1+j), \quad (9)$$

where

$$j = -\frac{1}{3}\left(\frac{X_u^+}{m^+} + \frac{M_q^+}{I_y^+}\right) \Bigg/ \sqrt[3]{\frac{g^+ M_u^+}{I_y^+}}. \quad (10)$$

The root of Eq. (7) is simply

$$\lambda_4^+ = \frac{Z_w^+}{m^+}. \quad (11)$$

Values of $\lambda_{1,2}^+$, λ_3^+, and λ_4^+ computed by the above approximate expressions, Eqs. (8)–(11), are shown in Table VI, compared with the exact values taken from Table V (the exact values are given in parentheses in Table VI). It is seen that the approximate values are almost equal to the corresponding exact values, showing that Eqs. (8)–(11) are very good approximations to the eigenvalues. Note that in the real part of $\lambda_{1,2}^+$ in Eq. (8) (the real part represents the growth rate of the instability), there are contributions from M_q and X_u; they are in the expression of j, Eq. (10). They are damping derivatives: M_q is the rotational damping of pitching rotation (rotational damping in flapping flight has been discussed in detail by Hedrick *et al.* [9]); X_u is damping of horizontal translational motion. Since M_q and X_u are negative, j will be positive; we see from Eq. (8) that the damping derivatives have the effect of decreasing the growth rate of the instability; i.e., they make instability slower.

Now, using the real part of Eq. (8), we can derive an analytical expression for t_d varying as a function of m as follows. Let ξ^+ be the real part of λ_1^+ (or λ_2^+) and $\xi = \xi^+/T = \xi^+ n$, and from Eq. (8) we have

$$\xi = \frac{1}{2}\sqrt[3]{\frac{M_u^+ g^+}{I_y^+}}(1-2j)n. \quad (12)$$

Introducing $g^+ = gT/U$, $m^+ = m/0.5\rho U S_t T$, and $I_y^+ = I_y/0.5\rho U^2 S_t c T^2$, Eq. (12) becomes

$$\xi = \frac{1}{2}\sqrt[3]{\frac{2M_u^+ g\rho\Phi r_2 c^2 R n}{m l_2^2}}(1-2j). \quad (13)$$

Letting l_2 and l_b represent the radius of gyration of insect mass about the y axes and the body length of the insect, respectively, Eq. (13) can be written as

$$\xi = \frac{1}{2}\sqrt[3]{M_u^+ g\rho\Phi\frac{r_2}{R}\left(\frac{l_2}{l_b}\frac{l_b}{R}\right)^{-2}\left(\frac{c}{R}\right)^2}\sqrt[3]{\frac{R^2 f}{m}}(1-2j). \quad (14)$$

In general, M_u^+, Φ, $\frac{r_2}{R}$, $\frac{l_2}{l_b}$, $\frac{l_b}{R}$, and $\frac{c}{R}$ do not vary greatly among the insects and we can assume that

$$\xi \propto \sqrt[3]{\frac{R^2 f}{m}}(1-2j). \quad (15)$$

TABLE VI. Eigenvalues computed by approximate expressions (the exact values are given in parentheses).

Species	Mode 1 λ_1, λ_2 (s^{-1})	Mode 2 λ_3 (s^{-1})	Mode 3 λ_4 (s^{-1})
Manduca sexta 1	$0.17 \pm 0.40i$ ($0.17 \pm 0.40i$)	-0.53 (-0.53)	-0.09 (-0.09)
Manduca sexta 2	$0.25 \pm 0.59i$ ($0.26 \pm 0.57i$)	-0.72 (-0.73)	-0.094 (-0.095)
Bombus terrestris 1	$0.045 \pm 0.13i$ ($0.042 \pm 0.13i$)	-0.20 (-0.19)	-0.012 (-0.011)
Bombus terrestris 2	$0.06 \pm 0.12i$ ($0.06 \pm 0.12i$)	-0.15 (-0.15)	-0.02 (-0.02)
Eristalis tenax	$0.047 \pm 0.094i$ ($0.047 \pm 0.093i$)	-0.11 (-0.11)	-0.015 (-0.015)
Episyrphus balteatus	$0.074 \pm 0.14i$ ($0.076 \pm 0.14i$)	-0.17 (-0.17)	-0.020 (-0.020)
Tipula obsolete	$0.33 \pm 0.73i$ ($0.36 \pm 0.72i$)	-0.87 (-0.88)	-0.11 (-0.11)
Cyrtodiopsis dalmanni	$0.05 \pm 0.11i$ ($0.05 \pm 0.11i$)	-0.13 (-0.13)	-0.02 (-0.02)
Drosophila virilis	$0.082 \pm 0.19i$ ($0.081 \pm 0.19i$)	-0.24 (-0.24)	-0.027 (-0.27)
Aedes aegypti (female)	$0.023 \pm 0.045i$ ($0.023 \pm 0.045i$)	-0.54 (-0.55)	-0.008 (-0.008)
Drosophila melanogaster	$0.067 \pm 0.14i$ ($0.067 \pm 0.14i$)	-0.18 (-0.18)	-0.024 (-0.024)
Aedes aegypti (male)	$0.018 \pm 0.036i$ ($0.018 \pm 0.034i$)	-0.044 (-0.42)	-0.007 (-0.007)
Liriomyza sativae	$0.11 \pm 0.24i$ ($0.11 \pm 0.24i$)	-0.30 (-0.30)	-0.014 (-0.014)
Anbremia sp.	$0.12 \pm 0.28i$ ($0.10 \pm 0.31i$)	-0.46 (-0.44)	-0.13 (-0.10)

It has been found that for many insects, R is proportional to $m^{0.36}$ and n is proportional to $m^{0.24}$ [1]; therefore Eq. (15) can be written as

$$\xi \propto m^{0.17}(1-2j). \tag{16}$$

The expression of j was given in Eq. (10). It can be written as

$$\begin{aligned} j &= -\frac{1}{3}\left(\frac{2X_u^+\rho\Phi r_2 cR}{m} + \frac{4M_q^+\rho\Phi^2 r_2^2 c^2 R}{ml_2^2}\right)\Bigg/ \sqrt[3]{\frac{2M_u^+ g\rho\Phi r_2 c^2 R}{ml_2^2 f^2}} \\ &= -\left[\frac{2}{3}\sqrt[3]{\frac{X_u^{+3}\rho^2\Phi^2}{2M_u^+ g}}\left(\frac{r_2}{R}\right)^2 \frac{c}{R}\left(\frac{l_2}{l_b}\frac{l_b}{R}\right)^2 \right. \\ &\quad \left. + \frac{4}{3}\sqrt[3]{\frac{M_q^{+3}\rho^2\Phi^5}{2M_u^+ g}}\left(\frac{r_2}{R}\right)^5\left(\frac{c}{R}\right)^4\left(\frac{l_2}{l_b}\frac{l_b}{R}\right)^{-4}\right]\sqrt[3]{\frac{R^7 f^2}{m^2}}. \end{aligned} \tag{17}$$

Again assuming X_u^+, M_u^+, Φ, $\frac{r_2}{R}$, $\frac{l_2}{l_b}$, $\frac{l_b}{R}$, and $\frac{c}{R}$ do not change greatly among the insects, Eq. (17) becomes

$$j \propto \sqrt[3]{\frac{R^7 f^2}{m^2}}; \tag{18}$$

i.e.,

$$j \propto m^{0.01}. \tag{19}$$

With Eq. (19), Eq. (16) can be written as

$$\xi \propto m^{0.17}(1 - bm^{0.01}), \tag{20}$$

where b is a constant. Since $m^{0.01}$ varies with m very slowly, $bm^{0.01}$ can be taken as a constant and Eq. (20) can be approximated as

$$\xi \propto m^{0.17}. \tag{21}$$

Thus t_d ($= 0.693/\xi$) can be written as

$$t_d = am^{0.17}, \tag{22}$$

where a is a constant. Using the data in Fig. 3 and applying the least squares method, a is determined as 38.37. The value of t_d computed using Eq. (22) is plotted in Fig. 4, compared with the data from Fig. 3. It is seen that Eq. (22) gives a good prediction on t_d varying as a function of m.

Equation (22) shows that t_d is proportional to the 0.17 power of the insect mass (m), which means that as the mass of the insect decreases, t_d will decrease (i.e., the instability becomes fast). This indicates that smaller insects need shorter reaction times than larger insects. Data on insect reaction time that could be found in the existing literature are limited to only three species of insects (fruit fly [24] and honey bee and stalk-eyed fly [35]). The reaction time of honey bee ($m \approx 102$ mg), stalk-eyed fly ($m \approx 7$ mg), and fruit fly ($m \approx 0.96$ mg) have been measured to be 20.3, 16.5, and 13 ms, respectively. These data show that smaller insects have shorter reaction times. This provides some support to our finding.

V. CONCLUSIONS

In the present study, the longitudinal flight dynamic stability of two hovering miniature insects was computed. With the computed stability properties of the miniature insects and those of large insects from previous works, we studied the effects of insect size on the longitudinal flight dynamic sta-

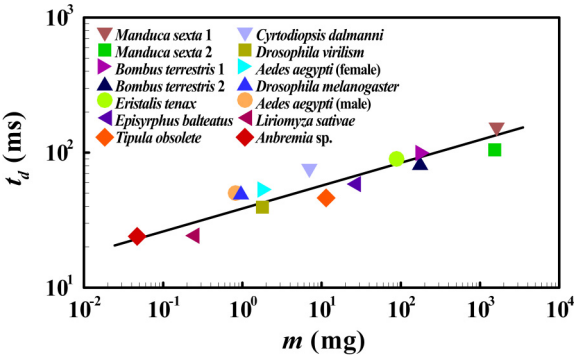

FIG. 4. The relationship between t_d and m.

TABLE VII. Parameters of two miniature insects. m: insect mass; h_1: distance between the center of mass and the middle of wing roots; h_1: distance between the middle of wing roots and the body axis; I_y: moment of inertia about the y axis.

Species	m (mg)	h_1 (mm)	h_2 (mm)	I_y (kg m^2)
Vegetable leaf miner (*Liriomyza sativae*)	0.25	0.30	0.18	4.85×10^{-14}
Gall midge (*Anbremia* sp.)	0.05	0.38	0.15	7.29×10^{-15}

bility of insects in the full range of insect sizes. We have the following results: Although the insects considered have a 30 000-fold difference in mass, their modal structure of flight stability is the same: There are an unstable oscillatory mode, a stable fast subsidence mode, and a stable slow subsidence mode; because of the unstable mode, the flight is unstable. An approximate analytical expression on the growth rate of the unstable mode as a function of insect mass (m) was derived. It shows that the time to double the initial values of disturbances (t_d) is proportional to the 0.17 power of the insect mass (m). That is, as m becomes smaller, t_d decreases (i.e., the instability becomes faster). This means that miniature insects need faster nervous systems to control the instability than larger insects. For example, the response time (represented by t_d) of a miniature insect, gall midge ($m \approx 0.05$ mg), needs to be faster by about 7 times than that of a larger insect, hawk moth ($m \approx 1600$ mg).

ACKNOWLEDGMENT

This research was supported by grants from the National Natural Science Foundation of China (Grants No. 11832004 and No. 11721202).

APPENDIX A: MORPHOLOGICAL PARAMETERS

In Eqs. (1) and (2), the insect mass and the moments of inertia are required. The mass of the vegetable leaf miner was measured and is available [30]. The mass of the miniature insect gall midge was not measured; it is estimated using the computed mean vertical force of the hovering insect, $m = \bar{F}_V/g$, where $\bar{F}_V$ is the mean vertical force computed by our group [29]. The measured mass of the vegetable leaf miner and the estimated mass of the gall midge are listed in Table VII. The moments and products of inertia were estimated using a method given by Ellington [2] and Zhang and Sun [18]. In the method, pictures of the side and dorsal vertical views of the body are obtained and the cross section of the body is taken as an ellipse, giving the body shape; a uniform density is assumed for the body. With these assumptions, the center of mass and the moments and products of inertia can be estimated. The results are also listed in Table VII.

APPENDIX B: CALCULATION OF THE STABILITY DERIVATIVES

In addition to the mass and the moments of inertia, the stability derivatives are also required in Eqs. (1) and (2). The detailed process of calculating the derivatives have appeared in several papers of our group (e.g., Refs. [8,18]). Only a brief description is given here. The wing flapping kinematics at hovering (equilibrium) flight is obtained from Refs. [29,30]; so is the wing geometry.

In determining the stability derivatives, the computational fluid dynamics method is used to compute the forces and moments; the method used to solve the Navier-Stokes equations is the same as that in Sun and Tang [36]. The hovering flight is taken as the reference flight in the calculation of the stability derivatives. A stability derivative is a partial derivative; e.g., X_u denotes the rate of change of X when only u is changed. In order to calculate the stability derivatives, six consecutive flow cases in which u, w, and q are varied separately are solved and the corresponding aerodynamic forces and moments are obtained. As an example, a u series means that u is varied while w and q are fixed at the reference values (i.e., $w = q = 0$); other series are similar to the u series.

Let ΔX^+, ΔZ^+, etc., denote the differences between X^+, Z^+, etc., and their corresponding values at hovering flight, respectively. The u-series, w-series, and q-series results of ΔX^+, ΔZ^+, and ΔM^+ are plotted. These curves, representing the variation of the aerodynamic forces and moments with each of the u, w, and q variables, are fitted and then the stability derivatives are estimated by the local tangent at the equilibrium point of the fitted curves.

[1] R. Dudley, *The Biomechanics of Insect Flight: Form, Function, Evolution* (Princeton University Press, Princeton, NJ, 2002).
[2] C. P. Ellington, The aerodynamics of hovering insect flight. II. Morphological parameters, Philos. Trans. R. Soc. London, Ser. B **305**, 17 (1984).
[3] T. L. Hedrick, S. A. Combes, and L. A. Miller, Recent developments in the study of insect flight, Can. J. Zool. **93**, 925 (2015).
[4] S. P. Sane, Neurobiology and biomechanics of flight in miniature insects, Curr. Opin. Neurobiol. **41**, 158 (2016).
[5] T. Weis-Fogh, Quick estimates of flight fitness in hovering animals, including novel mechanisms for lift production, J. Exp. Biol. **59**, 169 (1973).
[6] A. P. Willmott and C. P. Ellington, The mechanics of flight in the hawkmoth Manduca sexta. I. Kinematics of hovering and forward flight, J. Exp. Biol. **200**, 2705 (1997).
[7] G. K. Taylor and A. L. R. Thomas, Dynamic flight stability in the desert locust Schistocerca gregaria, J. Exp. Biol. **206**, 2803 (2003).
[8] M. Sun and Y. Xiong, Dynamic flight stability of a hovering bumblebee, J. Exp. Biol. **208**, 447 (2005).

[9] T. L. Hedrick, B. Cheng, and X. Deng, Wingbeat time and the scaling of passive rotational damping in flapping flight, Science **324**, 252 (2009).
[10] I. Faruque and J. S. Humbert, Dipteran insect flight dynamics. Part 1: Longitudinal motion about hover, J. Theor. Biol. **264**, 538 (2010).
[11] I. Faruque and J. S. Humbert, Dipteran insect flight dynamics. Part 2: Lateral–directional motion about hover, J. Theor. Biol. **265**, 306 (2010).
[12] H. Liu, T. Nakata, N. Gao, M. Maeda, H. Aono, and W. Shyy, Micro air vehicle-motivated computational biomechanics in bio-flights: Aerodynamics, flight dynamics and maneuvering stability, Acta Mech. Sin. **26**, 863 (2010).
[13] B. Cheng and X. Y. Deng, Translational and rotational damping of flapping flight and its dynamics and stability at hovering, IEEE Trans. Robot. **27**, 849 (2011).
[14] M. Sun, Insect flight dynamics: Stability and control, Rev. Mod. Phys. **86**, 615 (2014).
[15] Z. J. Wang, Insect Flight: From Newton's law to neurons, Annu. Rev. Condens. Matter Phys. **7**, 281 (2016).
[16] M. Sun, J. Wang, and Y. Xiong, Dynamic flight stability of hovering insects, Acta Mech. Sin. **23**, 231 (2007).
[17] N. Xu and M. Sun, Lateral flight stability of two hovering model insects, J. Bionic Eng. **11**, 439 (2014).
[18] Y. L. Zhang and M. Sun, Dynamic flight stability of a hovering model insect: Lateral motion, Acta Mech. Sin. **26**, 175 (2010).
[19] C. Shen, A study of the landing and vertically-ascending flight in fruitflies, Ph.D. thesis, Beihang University, 2018.
[20] L. G. Liu and M. Sun, Dynamic flight stability of hovering mosquitoes, J. Theor. Biol. **464**, 149 (2019).
[21] W. B. Dickson, A. D. Straw, and M. H. Dickinson, Integrative model of Drosophila flight, AIAA J. **46**, 2150 (2008).
[22] M. Sun and J. K. Wang, Flight stabilization control of a hovering model insect, J. Exp. Biol. **210**, 2714 (2007).
[23] L. Ristroph, A. J. Bergou, G. Ristroph, K. Coumes, G. J. Berman, J. Guckenheimer, Z. J. Wang, and I. Cohen, Discovering the flight autostabilizer of fruit flies by inducing aerial stumbles, Proc. Natl. Acad. Sci. USA **107**, 4820 (2010).
[24] L. Ristroph, G. Ristroph, S. Morozova, A. J. Bergou, S. Chang, J. Guckenheimer, Z. J. Wang, and I. Cohen, Active and passive stabilization of body pitch in insect flight, J. R. Soc. Interface **10**, 20130237 (2013).
[25] B. Cheng, X. Y. Deng, and T. L. Hedrick, The mechanics and control of pitching maneuvers in a freely flying hawkmoth (*Manduca sexta*), J. Exp. Biol. **214**, 4092 (2011).
[26] J. H. Wu and M. Sun, Floquet stability analysis of the longitudinal dynamics of two hovering model insects, J. R. Soc. Interface **9**, 74 (2012).
[27] R. M. Noest and Z. J. Wang, Optimal wing hinge position for fast ascent in a model fly, J. Fluid Mech. **849**, 498 (2018).
[28] S. Chang and Z. J. Wang, Predicting fruit fly's sensing rate with insect flight simulations, Proc. Natl. Acad. Sci. USA **111**, 11246 (2014).
[29] Y. Z. Lyu, H. J. Zhu, and M. Sun, Flapping-mode changes and aerodynamic mechanisms in miniature insects, Phys. Rev. E **99**, 012419 (2019).
[30] X. Cheng and M. Sun, Wing-kinematics measurement and aerodynamics in a small insect in hovering flight, Sci. Rep. **6**, 25706 (2016).
[31] X. Cheng and M. Sun, Very small insects use novel wing flapping and drag principle to generate the weight-supporting vertical force, J. Fluid Mech. **855**, 646 (2018).
[32] B. Etkin and L. D. Reid, *Dynamics of Flight: Stability and Control* (John Wiley & Sons Inc., New York, 1996).
[33] C. P. Ellington, The aerodynamics of hovering insect flight. III. Kinematics, Philos. Trans. R. Soc. London, Ser. B **305**, 41 (1984).
[34] R. Dudley and C. P. Ellington, Mechanics of forward flight in bumblebees. I. Kinematics and morphology, J. Exp. Biol. **148**, 19 (1990).
[35] J. T. Vance, I. Faruque, and J. S. Humbert, Kinematic strategies for mitigating gust perturbations in insects, Bioinspiration Biomimetics **8**, 016004 (2013).
[36] M. Sun and J. Tang, Unsteady aerodynamic force generation by a model fruit fly wing in flapping motion, J. Exp. Biol. **205**, 55 (2002).